R & D NOTES

A Deactivation Model for Bidispersed Catalysis

Timur Doğu
Faculty of Sciences
University of Ankara
Ankara, Turkey

Hülya Peker and Kurtul Küçükada
Middle East Technical University
Ankara, Turkey

A number of models were proposed in the literature for the prediction of deactivation rates of catalysts. Masamune and Smith (1966) analyzed the deactivation process by a shell model. Krishnaswamy and Kittrell (1981) and Zrncevic (1984) considered intraparticle deactivation processes. Diffusional influences were also included in the analysis by Krishnaswamy and Kittrell.

Many of the catalyst pellets are made by the agglomeration of small microporous particles. Such catalysts have a bidispersed pore structure. It was shown by Örs and Doğu (1979) that, for a bidispersed catalyst pellet, the effectiveness factor was a function of particle Thiele Modulus (Φ_i) and a dimensionless group α. This group is proportional to the ratio of diffusion times in the macro- and micropore regions of the pellet. Kulkarni et al. (1981) and Jayaraman et al. (1983) extended this approach to nonlinear rate expressions. Küçükada and Doğu (1985) generalized the effectiveness factor expression for bidispersed catalysts for different geometries and with respect to α. Dilution of active material in bidispersed catalysts was investigated by John and Varghese (1985a,b). Datar et al. (1986, 1987) extended the Örs and Doğu approach to systems with diffusivity variations and to nonisothermal systems. Maheshwari et al. (1985) investigated the deactivation of bidispersed catalysts assuming a simple, first-order, concentration-independent deactivation mechanism and predicted the variation of effectiveness factor for this mechanism. In this mechanism, the deactivation rate was considered to be uniform throughout the pellet and did not depend on the position.

The objective of the present study was to develop a particle-pellet model for the deactivation of bidispersed catalysts in which position dependence of activity within the pellet was taken into consideration. It was shown that the effectiveness factor passed through a maximum at a certain Thiele modulus, especially at large times. The significance of α on the deactivation rate was also illustrated.

Particle-Pellet Deactivation Model

It was considered in this model that a bidispersed catalyst pellet was composed of microporous particles and macropores between the agglomerated particles. The surface area of micropores is much greater than the macropore surface area and most of the active sites lie within the microporous region. Considering these factors, the microporous particles were taken to be composed of two regions: deactivated shell and active core regions, Figure 1. For a parallel deactivation process, the pseudosteady-state, dimensionless species conservation equations were written in the active core and deactivated shell regions of a spherical microporous particle.

Active core region (microporous particle):

$$\frac{1}{\xi^2}\frac{d}{d\xi}\left(\xi^2\frac{d\psi_c}{d\xi}\right) = \Phi_i^2\psi_c, \quad 0 \le \xi \le \xi_i \tag{1}$$

Deactivated shell region (microporous particle):

$$\frac{1}{\xi^2}\frac{d}{d\xi}\left(\xi^2\frac{d\psi_s}{d\xi}\right) = 0, \quad \xi_i \le \xi \le 3 \tag{2}$$

In writing these equations, a first-order *chemical* reaction was considered. Similarly, the species conservation equation for a spherical pellet was expressed as,

$$\frac{1}{\lambda^2}\frac{d}{d\lambda}\left(\lambda^2\frac{d\psi_a}{d\lambda}\right) - \alpha\left(\frac{d\psi_s}{d\xi}\right)_{\xi=3} = 0 \tag{3}$$

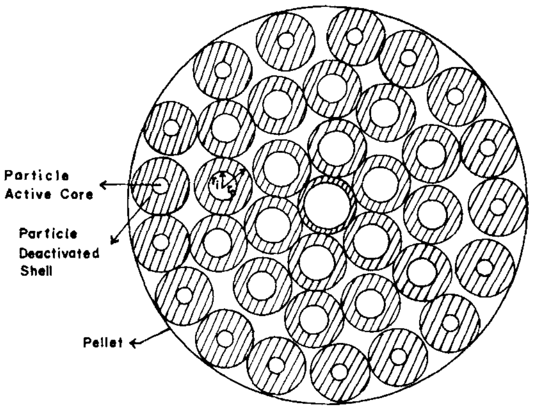

Figure 1. Schematic representation of a deactivating bidispersed catalyst pellet.

where the dimensionless groups Φ_i and α were defined as:

$$\Phi_i = \frac{r_o}{3}\left(\frac{\varrho'_p S k_s}{D_i}\right)^{1/2} \tag{4}$$

$$\alpha = (1 - \epsilon_a)\frac{D_i}{D_a}\frac{R_o^2}{r_o^2} \tag{5}$$

For this model, the boundary conditions were expressed as follows.

Particle boundary conditions:

$$\psi_s = \psi_a \quad \text{at } \xi = 3 \tag{6}$$

$$\psi_s = \psi_c \quad \text{at } \xi = \xi_i \tag{7}$$

$$\frac{d\psi_c}{d\xi} = 0 \quad \text{at } \xi = 0 \tag{8}$$

$$\delta\frac{d\psi_c}{d\xi} = \frac{d\psi_s}{d\xi} \quad \text{at } \xi = \xi_i \tag{9}$$

Pellet boundary conditions:

$$\psi_a = 1 \quad \text{at } \lambda = 3 \tag{10}$$

$$\frac{d\psi_a}{d\lambda} = 0 \quad \text{at } \lambda = 0 \tag{11}$$

In these equations, ξ_i corresponds to the dimensionless position of the boundary between the active core and the deactivated shell regions of the particle. The value of ξ_i varies with position in the pellet and with time. The dimensionless parameter δ corresponds to the ratio of micropore diffusion coefficients in the active core and the deactivated shell regions of the particle. Assuming that the pore structure of the active core and the deactivated shell regions of the catalyst particles were not very much different, the value of this parameter was taken as unity in the following analysis. For systems with significant diffusivity changes due to deactivation, the analysis should be repeated with appropriate δ values.

The solution of Eqs. 1 and 2 with the boundary conditions given in Eqs. 6, 7, 8 and 9 gave the concentration profile expressions in the shell and core regions of a partially deactivated particle.

$$\psi_s = \frac{\psi_a\left\{1 - \xi_i\left(\frac{\xi_i}{\xi} - 1\right)\Phi_i\left[\frac{1}{\tanh(\Phi_i\xi_i)} - \frac{1}{\Phi_i\xi_i}\right]\right\}}{1 - \xi_i\left(\frac{\xi_i}{3} - 1\right)\Phi_i\left[\frac{1}{\tanh(\xi_i\Phi_i)} - \frac{1}{\Phi_i\xi_i}\right]} \tag{12}$$

$$\psi_c = \frac{\xi_i}{\xi} \cdot \frac{\sinh(\Phi_i\xi)\psi_a}{\sinh(\Phi_i\xi_i)\left[1 - \xi_i\left(\frac{\xi_i}{3} - 1\right)\Phi_i\left(\frac{1}{\tanh(\Phi_i\xi_i)} - \frac{1}{\Phi_i\xi_i}\right)\right]} \tag{13}$$

The concentration gradient at the external surface of the deactivating microporous particle was then evaluated as

$$\left(\frac{d\psi_s}{d\xi}\right)_{\xi=3} = \psi_a f(\xi_i, \Phi_i) \tag{14}$$

where,

$$f(\xi_i, \Phi_i) = \frac{(\xi_i/3)^2\Phi_i\left[\frac{1}{\tanh(\Phi_i\xi_i)} - \frac{1}{(\Phi_i\xi_i)}\right]}{1 - \xi_i\left(\frac{\xi_i}{3} - 1\right)\Phi_i\left[\frac{1}{\tanh(\Phi_i\xi_i)} - \frac{1}{(\Phi_i\xi_i)}\right]} \tag{15}$$

Equation 14 was then substituted into Eq. 3.

$$\frac{1}{\lambda^2}\frac{d}{d\lambda}\left(\lambda^2\frac{d\psi_a}{d\lambda}\right) - \alpha\psi_a f(\xi_i, \Phi_i) = 0 \tag{16}$$

The evaluation of concentration profile in the pellet and consequently the effectiveness factor expression require the solution of this equation. For this integration, it is necessary to have some knowledge about the dependence of ξ_i on λ.

Following a similar approach as Masamune and Smith, the movement of the boundary between the active core and the deactivated shell regions was related to the total poisoning reaction within the particle. For a first-order deactivation process, the rate of change of ξ_i with respect to time can be written as,

$$-\xi_i^2\frac{d\xi_i}{d\theta} = \int_0^{\xi_i}\xi^2\psi_c\,d\xi \tag{17}$$

where,

$$\theta = \frac{k_d C_o t}{Q_o} \tag{18}$$

Equations 13 and 17 were then combined to obtain,

$$-\frac{d\xi_i}{d\theta} = \psi_a\frac{\left[\frac{1}{\Phi_i\tanh(\Phi_i\xi_i)} - \frac{1}{\Phi_i^2\xi_i}\right]}{\left[1 - \xi_i\left(\frac{\xi_i}{3} - 1\right)\Phi_i\left\{\frac{1}{\tanh(\Phi_i\xi_i)} - \frac{1}{\Phi_i\xi_i}\right\}\right]} \tag{19}$$

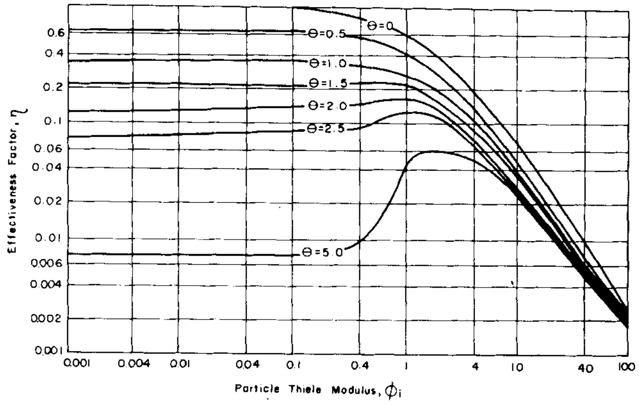

Figure 2a. $\alpha = 0.1$.

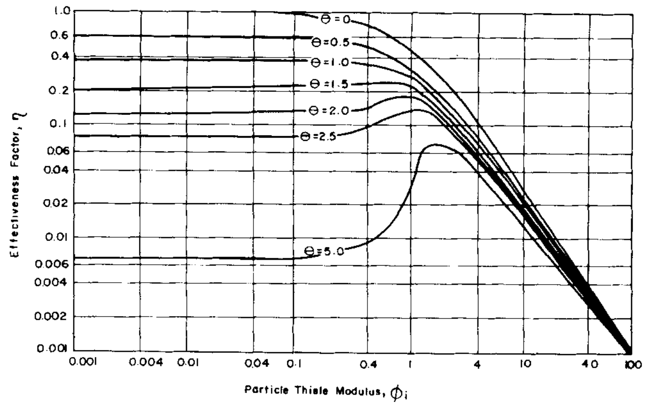

Figure 2b. $\alpha = 1.0$.

This equation shows that ξ_i is a function of particle Thiele modulus (Φ_i), dimensionless time, θ, and macropore concentration profile, ψ_a. As the diffusion resistance in the macropores becomes significant, the dependence of ψ_a on λ and consequently the dependence of ξ_i on λ increase. The evaluation of concentration profile in the pellet requires the simultaneous solution of Eq. 16 with Eq. 19.

Effectiveness Factor for the Deactivating Pellet

The effectiveness factor for a bidispersed catalyst was derived from the diffusion flux at the external surface of the pellet.

$$\eta = \frac{1}{\Phi_i^2 \alpha} \left(\frac{d\psi_a}{d\lambda} \right)_{\lambda-3} \tag{20}$$

By integrating Eq. 3, the concentration gradient at the external surface of the macroporous pellet was evaluated and then the effectiveness factor was expressed (Küçükada, 1986).

$$\eta = \frac{\sqrt{2}}{9\Phi_i^2 \alpha^{1/2}} \left[\int_{\psi_{a_c}}^{1} \left(\frac{d\psi_s}{d\xi} \right)_{\xi-3} \lambda^4 \, d\psi_a \right]^{1/2} \tag{21}$$

$$= \frac{1}{9\Phi_i^2} \int_0^3 \left(\frac{d\psi_s}{d\xi} \right)_{\xi=3} \lambda^2 \, d\lambda \tag{22}$$

If macropore diffusion is not limiting, which corresponds to small values of α, the integration of these equations together with Eq. 14 gives.

$$\eta = \frac{1}{\Phi_i^2 \alpha} \left[\frac{(\alpha f(\xi_i, \Phi_i))^{1/2}}{\tanh\,(3(\alpha f(\xi_i, \Phi_i))^{1/2})} - \frac{1}{3} \right] \tag{23}$$

where $f(\xi_i, \Phi_i)$ is given by Eq. 15.

The general solution of the model equations requires numerical analysis. Equations 14, 16 and 19 were solved by using a finite-difference method and value of $d\psi_a/d\lambda$ was estimated at the external surface of the pellet. Then, effectiveness factor values were calculated for different Φ_i, α, and θ values.

Results and Discussion

The variation of effectiveness factor as a function of particle Thiele Modulus and dimensionless time is illustrated in Figures 2a and 2b for $\alpha = 0.1$ and $\alpha = 1.0$, respectively. The results showed that, for lower values of the particle Thiele Modulus, Φ_i, deactivation is faster than the diffusion-controlling region. As a result, rate of decrease of η with time is faster at small Φ_i values as compared to higher Φ_i values. On the other hand, the reaction rate at high Thiele Modulus is intrinsically lower than the reaction rate at low Thiele Modulus. As a result of these two factors, effectiveness factor passes through a maximum between the kinetics- and diffusion-controlling regions. For higher values of the particle Thiele modulus, the effectiveness factor curves converge.

The increase of the values of the parameter α has very small effect on the effectiveness factor for low values of the Thiele Modulus, Figure 3. On the other hand, the effect of α becomes more and more significant as the value of Φ_i increases. The variation of η with Φ_i at different α values is given in Figure 3 for a typical value of dimensionless time, $\theta = 2.5$. For larger values of α, diffusion resistance in the macropores is larger than the diffusion resistance in the micropores. As a result, the magnitude of effectiveness factor becomes smaller as α increases. This effect is significant especially at high Thiele modulus values. The analysis indicated that the life of the catalyst is longer for larger values of α as well as for large values Φ_i.

Notation

C_a = concentration of reactant A in the macropores
C_i = concentration of reactant A in the micropores

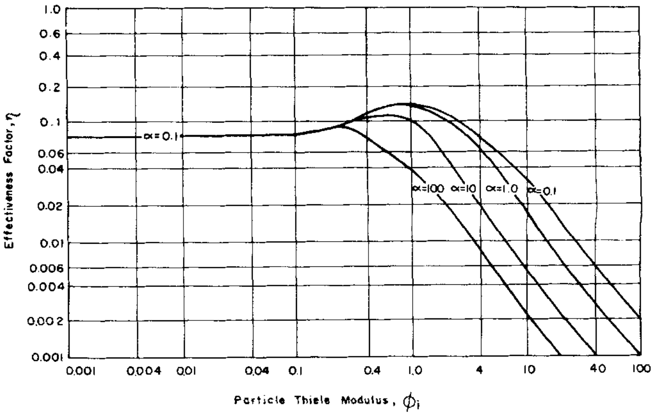

Figure 3. Variation of effectiveness factor with Thiele Modulus at $\theta = 2.5$ for different values of α.

C_o = external surface concentration of A
D_a = effective macropore diffusion coefficient
D_i = effective micropore diffusion coefficient
k_s = surface reaction rate constant
k_d = deactivation rate constant
Q_o = concentration of deposited material per unit volume of catalyst pellet
R = diffusion coordinate in the pellet
R_o = pellet radius
r = diffusion coordinate in the particle
r_i = radial position of the boundary between the active core and deactivated shell sections of a particle
r_o = particle radius
S = surface area per unit mas of catalyst
t = time

Greek letters

α = dimensionless parameter defined by Eq. 5
ϵ_a = macroporosity of the pellet
η = pellet effectiveness factor
$\rho_p = \rho_p'(1 - \epsilon_a)$ pellet density
ρ_p' = particle density
Φ_i = particle Thiele modulus defined by Eq. 4
ψ_a = dimensionless concentration in the macropores, C_a/C_o
ψ_c = dimensionless concentration in the active core micropores
ψ_s = dimensionless concentration in the deactivated shell micropores
ξ = dimensionless coordinate in the particle, $r/(r_o/3)$
λ = dimensionless coordinate in the pellet, $R/(R_o/3)$
θ = dimensionless time, defined by Eq. 18

Literature Cited

Datar, A. S., B. D. Kulkarni, and L. K. Doraiswamy, "Effectiveness Factors in Bidispersed Catalysts under Nonisothermal Conditions," *AIChE J.*, **32**, 859 (1986).

Datar, A. S., B. D. Kulkarni, and L. K. Doraiswamy, "Effectiveness Factors in Bidispersed Catalysts, The Effect of Diffusivity Variations," *Chem. Eng. Sci.*, **42**, 1233 (1987).

Jayaraman, V. K., B. D. Kulkarni, and L. K. Doraiswamy, "A Simple Method for the Solution of a Class of Reaction Diffusion Problems," *AIChE J.*, **29**, 521 (1983).

John, V., and P. Varghese, "A Bidispersed Porosity Approach in Dilution in Catalyst Pellets with Uniform Distribution of Active Material," *AIChE J.*, **32**, 1216 (1986a).

John, V., and P. Varghese, "Dilution of Active Material in Catalyst Pellets, Design Criteria for Optimal Performance," *Chem. Eng. Sci.*, **41**, 725 (1986b).

Krishnaswamy, S., and J. R. Kittrell, "Diffusional Influences on Deactivation Rates," *AIChE J.*, **27**, 120 (1981).

Kulkarni, B. D., V. K. Jayaraman, and L. K. Doraiswamy, "Effectiveness Factors in Bidispersed Porous Catalysts: The General nth Order Case," *Chem. Eng. Sci.*, **36**, 943 (1981).

Küçükada, K., "Modelling of Deactivation in Bidisperse Catalysts," M. S. Thesis, Middle East Technical University, Ankara, Turkey (1985).

Küçükada, K., and T. Doğu, "A Note on Generalization of Effectiveness Factor for Bidispersed Porous Catalysts," *AIChE J.*, **31**, 2086 (1986).

Maheshwari, V., S. C. Nigam, and D. Kunzru, "Diffusional Influences on Deactivation Rates of Bidispersed Catalysts," **31**, 1393 (1985).

Masamune, S., and J. M. Smith, "Performance of Fouled Catalyst Pellets," *AIChE J.*, **12**, 385 (1966).

Örs, N., and T. Doğu, "Effectiveness of Bidispersed Catalysts," *AIChE J.*, **25**, 723 (1979).

Zrncevic, S., "The Intraparticle Deactivation of Ni-SiO_2-Al_2O_3 by Thiophene in Benzene Hydrogenation," *Chem. Eng. Sci.*, **39**, 1245 (1984).

Manuscript received Feb. 22, 1988, and revision received May 24, 1988.